



# The effects of physical aging on the quasi-static and dynamic viscoelastic properties of Nitrile Butadiene Rubber

Syam Prasad Ammineni<sup>1,2</sup> · D. Lingaraju<sup>1</sup> · Ch. Nagaraju<sup>3</sup>

Received: 12 December 2022 / Accepted: 20 February 2023 / Published online: 16 March 2023  
© The Author(s), under exclusive licence to Springer Nature B.V. 2023

## Abstract

The effect of physical natural aging of nitrile butadiene rubber (NBR) on the degradation of its viscoelastic properties was investigated in both time and frequency domains. Quasi-static and dynamic mechanical tests were conducted on virgin and naturally aged NBR specimens to analyse their structural integrity for damping applications. The generalized Maxwell model was used to fit the Dynamic Mechanical Analysis (DMA) experimental data to determine the deterioration of the constitutive viscoelastic parameters with age. Fourier transform infrared spectroscopy (FTIR) was used to investigate the aging of functional groups in NBR. Thermogravimetric Analysis (TGA) was performed to estimate the changes in the activation energy and frequency factor with age to estimate the shelf life of the NBR. The structural damping characteristics of the NBR were analyzed using an unconstrained sandwich beam with NBR and aluminum as the base material. According to experimental results, the mechanical properties deteriorated by approximately 43%. With age, constitutive viscoelastic properties, such as the storage modulus (52%), loss modulus (66%), loss factor (31%), and damping coefficient (31.25%) deteriorated. The relaxation strength and modulus decreased by 41.2% and 43.9%, respectively. The activation energy at higher conversion rates decreased from 529.77 kJ mol<sup>-1</sup> to 280.15 kJ mol<sup>-1</sup> for aged NBR. After two years, the damping ability of the aged NBR sandwich beam decreased by 8, 34, and 22% at the first three natural frequencies compared to virgin NBR sandwich beam.

**Keywords** DMA · FTIR · Maxwell · NBR · TGA

## 1 Introduction

Nitrile Butadiene Rubber (NBR) is a widely used polymer in damping and sealing applications due to its good mechanical and physical properties. It is polymerization of acrylonitrile and butadiene (40/60). However, over time and under certain environmental conditions,

---

✉ S.P. Ammineni  
[syampnaidu@gmail.com](mailto:syampnaidu@gmail.com)

<sup>1</sup> Department of Mechanical Engineering, JNTU Kakinada 533003, India

<sup>2</sup> Department of Mechanical Engineering, Maturi Venkata Subba Rao (MVSRR) Engineering College, Hyderabad, Telangana, 501510, India

<sup>3</sup> Department of Mechanical Engineering, Velagapudi Ramakrishna Siddhartha Engineering College, Kanuru, Vijayawada, Andhra Pradesh, 520007, India

NBR can degrade and lose its viscoelastic properties. Estimating the degradation in NBR's damping effectiveness with age and temperature is crucial in damping applications (Peng et al. 2019; Bendjaouahdou and Bensaad 2018; Feng et al. 2014; Choi and Kim 2012; Lyu et al. 2018; Ge et al. 2021; Vašina et al. 2018). Viscoelastic materials deform in shear mode during vibration dampening and dissipate energy in the form of heat to create an opposing force (Lakes 2009). The viscoelastic properties of NBR can be measured using Dynamic Mechanical Analysis (DMA), which measures the loss modulus, an indicator of energy dissipation. According to viscoelastic fundamental principles, under cyclic loading, energy is dissipated by the viscous elements, and thus the applied stress and resulting strain have the same frequency with a certain phase lag (Jones 2001). Studies have been conducted to investigate the degradation of viscoelastic properties of naturally aged polymers under no-load conditions.

The physical aging of polymers has been extensively studied by Struik (1978) and experimentally analysed the changes in their engineering properties with age. Ko and Forsman (1980) modified the Weissenberg rheogoniometer to estimate the loss and storage modulus of viscoelastic solids under free and forced vibrations. Woo et al. (2010) predicted the useful lifetime of NBR and EPDM materials using an accelerated aging technique in a thermo-oxidative environment. The results showed that the polymer stiffness increased with age and the activation energy varied with time and temperature. NBR exhibited greater changes in constitutive viscoelastic properties than EPDM. Rajesh et al. (2021) investigate the changes in the dynamic mechanical properties of NBR with nylon 6. The experimental results showed that the curing agents had a greater influence on the dynamic mechanical properties. Jung et al. (2020) estimated the frequency-dependent viscoelastic material properties below room temperature in shear mode. Ranaei and Aghakouchak (2022) investigated the dynamic mechanical properties of elastomeric materials under harmonic loading. The results showed that the dynamic properties of viscoelastic materials are frequency- and strain-dependent. Qian et al. (2018) conducted aging tests on an NBR submerged in transformer oil under compressive loads at different operating temperatures and predicted its shelf life. Musil et al. (2020) in their research paper proposed a continuum mechanical model to predict the deterioration of dynamic mechanical properties of the NBR in air and oil environment. Nait Abdelaziz et al. (2019) worked on new developments in the area of fracture of rubbers and the influence of aging on mechanical properties. The stress limiter and energy limiter approaches were used to determine the failure stress and strain in elastomers under uniaxial tension. Esmaeeli and Farhad (2020) measured the viscoelastic properties of SBR using the new HFDMA technique in the range of 100 Hz–5 kHz. The experimental results were 5–7% more accurate than those of normal conventional methods. Liu et al. (2016) concluded that aging is caused by the surface damage of NBR, which makes the material inhomogeneous. Polukoshko (2016) estimated the damping properties of elastomers using mathematical and analytical models under harmonic excitation. Şen et al. (2020) investigated the effects of ionizing radiation on the mechanical properties of NBR/lignin elastomers and concluded that lignin protected the mechanical properties of NBR elastomers against irradiation. Gupta et al. (2004) investigated the degradation of thermoplastics with temperature and oxygen using Wall and Flynn techniques. Zhang (2020) summarise various kinetic methods for estimating the activation energy from TGA experiments. Chakraborty et al. (2007) proposed a method for identifying the functional groups of nitrile rubber using FTIR.

Previous studies (Tang and Zhang 2014; Xiong et al. 2013; Nakagawa et al. 1992; Zheng et al. 2017; Plota and Masek 2020; Maxwell et al. 2005; Ozawa 1965; Hussain et al. 2020; Abdullah et al. 2022; Li et al. 2021; Pertin et al. 2020) have used different accelerated aging techniques to study how environmental conditions affect polymers. This study specifically

examines the natural aging of NBR under no-load conditions in a laboratory setting for two years. It compares the virgin samples with the same chemical, physical, and mechanical properties. Mechanical properties such as tensile strength, young’s modulus, elongation break, density, and hardness were evaluated for both virgin and aged NBR samples. DMA and thermogravimetric analysis methods were used to determine the viscoelastic properties of NBR. FTIR tests were performed to identify the changes in functional groups that occur with aging. The study also used an unconstrained sandwich beam to measure the degradation of mechanical, modal parameters (natural frequency, damping, frequency response functions) of the NBR and to determine the damping characteristics of the virgin and aged NBR.

### 1.1 Theory of viscoelastic damping

The stress-strain response of polymers is time-dependent (Lakes 2009). For example, in damping and sealing applications, if a compressive load is suddenly applied and held at a fixed value, the strain will begin from zero, unlike at a rapid rate in elastic solids. The cyclic shear load and its response (Jones 2001) can be written as

$$\tau(t) = G\phi(t) \pm G\eta\sqrt{\phi_o^2 - \phi(t)^2} \tag{1}$$

where  $\tau(t)$  is shear stress,  $\phi(t)$  is shear strain,  $\phi_o$  is the maximum amplitude of the strain response in a cycle. For steady-state sinusoidal harmonic load, the response of shear strain can be written as

$$\phi(t) = \phi_o \sin(\omega t) \tag{2}$$

Where  $\omega$  is sinusoidal frequency in rad/sec, and substitute the equation (1) in equation (2)

$$\tau(t, \omega) = \tau_o \sin(\omega t + \delta) \tag{3}$$

$$\tau(t, \omega) = \phi_o [G'(\omega) \sin(\omega t) + G''(\omega) \cos(\omega t)] \tag{4}$$

$$\frac{\tau(t, \omega)}{\phi_o} = [G'(\omega) \sin(\omega t) + G''(\omega) \cos(\omega t)] \tag{5}$$

$$G^*(\omega) = G'(\omega) + iG''(\omega) \tag{6}$$

Where  $G^*(\omega)$  is the complex modulus,  $G'(\omega)$  is storage modulus that represents elastic behaviour and  $G''(\omega)$  is the loss modulus, which represents viscous behaviour. The ratio of loss modulus to storage modulus gives a loss factor  $\eta$

$$\eta = \frac{G''}{G'} = \tan \delta \tag{7}$$

When polymers are used as vibration isolators, the dynamic response of a single degree of freedom of viscoelastic materials subjected to external dynamic forces in the time domain is a function of phase lag  $\delta$  and can be written as (Jones 2001)

$$\eta = \tan \delta = 2\xi \tag{8}$$

The damping ability of a viscoelastic isolator depends on the damping ratio ( $\xi$ ) and specific damping capacity ( $\Psi$ ), which are functions of phase lag ( $\delta$ ) in the viscoelastic material

response. In steady-state harmonic excitation, the factors damping ratio ( $\xi$ ) and specific damping capacity ( $\Psi$ ) represent the damping ability of the viscoelastic material, which is defined as the ratio of energy dissipation to energy stored in a cycle. These constitutive damping parameters can be estimated using the 3 dB method at resonance frequencies ( $\omega_0$ ) by considering two offset frequencies with amplitudes  $\sqrt{2}$  on either side of the resonance frequency ( $\omega_1 < \omega_0, \omega_2 > \omega_0$ ) (Martinez-Agirre and Elejabarrieta 2011; Zhang and Hoshino 2019). For linear systems, specific damping capacity can be written (Graesser and Wong 1991)

$$\Psi = 2\pi \tan \delta = 2\pi \frac{\omega_2 - \omega_1}{\omega_0} \quad (9)$$

Along with the damping ratio ( $\xi$ ) and specific damping capacity ( $\Psi$ ), other dimensionless parameters that describe the damping characteristics of viscoelastic materials is logarithmic decrement ( $\Delta$ ), and quality factor ( $Q$ ), which are also function of phase lag ( $\delta$ ). Logarithmic decrement gives the relative degree of the energy dissipation or damping of the material that represents the rate at which the amplitude of vibrations decays, and it can be written as in Corsaro and Sperling (1990). The quality factor indicates how well the oscillations at the resonance frequency can be dampened by releasing energy. This is inversely correlated with the damping capacity. It is reciprocal of loss factor.

The damping ratio, specific damping capacity, and logarithmic decrement of a viscoelastic material are directly proportional to the loss factor ( $\eta$ ), which is constitute viscoelastic property that is significantly influenced by time and temperature.

## 1.2 Mechanical models of viscoelastic materials

Viscoelastic materials can be modelled using spring-dashpot systems, which consist of a spring representing elastic behaviour and a dashpot representing viscous behaviour. The Maxwell model and the Kelvin-Voigt model are the two basic models used to understand the time-dependent behaviour of viscoelastic materials. However, these models have limitations and cannot fully capture the dynamic behaviour of viscoelastic materials. For example, the Maxwell model focuses on viscoelastic fluid relaxation, while the Kelvin-Voigt model is simpler and only considers viscoelastic solid behaviour. Both models are also limited to a narrow frequency range, as they only examine relaxation with one relaxation time (Funk et al. 2009; Roylance 2001). To overcome these limitations, a Generalized Maxwell Model (GMM) is used in the present work, which combines an infinite number of elements to represent the relaxation behaviour more accurately at multiple frequencies. The GMM is a more robust model that can be fitted to experimental data to derive the time-dependent relaxation modulus  $G(t)$  using Equation (10).

$$G(t) = \sum_{i=1}^n G_i e^{-t/\tau_i} \quad (10)$$

For viscous materials, when  $t = 0$ , relaxation modulus  $G(t) = 0$ , and for elastic materials  $t = \infty$ , relaxation modulus is a finite value  $G(t) = G_e$ . However, for viscoelastic materials, which have both viscous and elastic components, and after a long time, the macromolecules flow and the stresses relax, resulting in elastic behaviour and the relaxation modulus is a finite value and can be estimated from Equation (11) (Ferry 1980; Williams et al. 1961)

$$G(t) = G_e + \sum_{i=1}^n G_i e^{-t/\tau_i} \quad (11)$$

The parameters,  $G_e$ ,  $G_i$ , and  $\tau_i$  in Equation (11) are known as Maxwell parameters, popularly known as Prony Series. Estimating the Maxwell model parameters ( $G_e$ ,  $G_i$ ,  $\tau_i$ ) in the time domain is difficult, therefore the time-domain equation can be written in the frequency domain for the storage modulus ( $G'(\omega)$ ) and loss modulus ( $G''(\omega)$ ) separately and is given by Tschoegl (1989).

$$G'(\omega) = G_e + \sum_{i=1}^n \frac{G_i \omega^2 \tau_i^2}{1 + \omega^2 \tau_i^2} \tag{12}$$

$$G''(\omega) = \sum_{i=1}^n \frac{G_i \omega \tau_i}{1 + \omega^2 \tau_i^2} \tag{13}$$

The Maxwell model parameters  $G_e$ ,  $G_i$  and  $\tau_i$  evaluated in the frequency and time domains were the same. To obtain precise curve fitting for the experimental data at lower frequencies, the first, second, and third order were taken ( $i = 3$ ) (Baumgaertel and Winter 1989) in the present work. From these Maxwell model constants, another parameter, called relaxation strength ( $\nabla$ ), can be calculated using Equation (14). It is the ratio of relaxation stiffness to relaxed stiffness and is a dimensionless parameter.

$$\nabla = \frac{G_i}{G_e} \tag{14}$$

### 1.3 Model-free kinetic methods

Modal-free kinetic methods are promising for determining the activation energy in polymers. In the present work, the Kissinger-Akahira-Sunose (KAS) and Ozawa-Flynn-Wall (OFW) models were used. These models do not follow any kinetic model, assuming that the thermokinetic reaction is a function of temperature at any given constant conversion rate. OFW and KAS follow a first-order isothermal kinetic degradation process, which requires conducting TGA experiments with at least three heating rates. The kinetic reaction rate, which depends on the conversion rate ( $\frac{d\theta}{dt}$ ), and is a function of temperature ( $T$ ) and was selected from the TGA experimental data (Zhang 2020).

$$\frac{d\theta}{dt} = \alpha \frac{d\theta}{dT} = K(T) h(\theta) \tag{15}$$

where,  $T$  is the decomposition temperature in Kelvin,  $h(\theta)$  is the isothermal kinetic model,  $\theta$  is the heating rate in °C/min, and  $K(T)$  is the Arrhenius rate constant, which is temperature-dependent and can be determined using the Arrhenius law from Equation (16).

$$K(T) = A e^{-\left(\frac{E_a}{RT}\right)} \tag{16}$$

where  $A$  is the pre-exponential or frequency factor,  $E_a$  is the activation energy, and  $R$  is the real gas constant (8.314 J/mol K).

From Equations (15) and (16), by applying the boundary conditions;  $\theta \rightarrow 0$  at  $T \rightarrow T_0$  becomes

$$H(\theta) = \int_0^\theta \frac{d\theta}{h(\theta)} = \int_{T_0}^T \frac{A}{\alpha} e^{-\left(\frac{E_a}{RT}\right)} dT = \frac{AE_a}{\theta R} P(\chi) \tag{17}$$

In Equation (18),  $\chi$  is equal to the exponential factor in Equation (16)  $\frac{E_a}{RT}$ ; different isothermal kinetic models are provided by the  $P(\chi)$  solution (Zhu et al. 2015).

### 1.3.1 Ozawa-Flynn-Wall (OFW) method

OFW method follows Doyle's approximation (Doyle 1965) that follows first-order isothermal kinetics and by which  $P(\chi)$  can be achieved as

$$\ln(P(\chi)) = \ln\left(\frac{E_a}{RT}\right) \cong -2.315 + \frac{E_a}{RT} \quad (18)$$

From Equations (16) and (18)

$$\ln(\alpha) = \ln\left(\frac{AE_a}{H(\theta)R}\right) - 2.315 - 0.4567\left(\frac{E_a}{RT}\right) \quad (19)$$

The Equation (19) can be re arranged as

$$E_a = -\frac{R}{0.4567} \left[ \frac{d(\ln\alpha)}{d(1/T)} \right] \quad (20)$$

Equation (20) gives the activation energy from OFW method and can be obtained from slope of  $\ln\alpha$  vs.  $1/T$  plot at different heating rates (Ozawa 1965; Flynn and Wall 1966).

### 1.3.2 Kissinger-Akahira-Sunose (KAS) method

KAS method follows Coats–Redfern approximation (Kissinger 1956; Akahira and Sunose 1971) to find the isothermal kinetic model  $P(\chi)$  and can be achieved as

$$P(\chi) \cong \left(\frac{E_a}{RT}\right)^{-2} e^{-\left(\frac{E_a}{RT}\right)} \quad (21)$$

From Equations (17) and (21)

$$\ln\left(\frac{\alpha}{T^2}\right) = \ln\left(\frac{AR}{E_a H(\theta)}\right) - \frac{E_a}{RT} \quad (22)$$

The Equation (22) can be re arranged as

$$E_a = -R \left[ \frac{d(\ln(\frac{\alpha}{T^2}))}{d(\frac{1}{T})} \right] \quad (23)$$

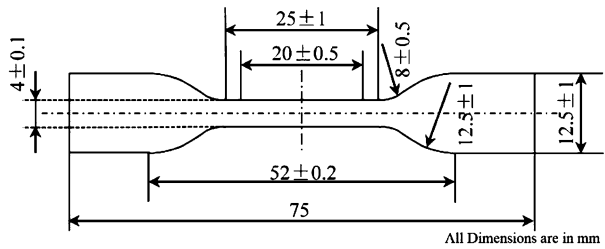
The slope of  $\ln(\frac{\alpha}{T^2})$  vs  $1/T$  plot gives the activation energy from the KAS method at different heating rates and provides accurate results for complex thermal decomposition reactions (Zhang 2020).

## 1.4 Life estimation

Shelf-life prediction and the estimation of polymers in damping applications are very important. The activation energy obtained from isothermal modal free kinetics was used at different conversation rates. At the given operating temperature ( $T_f$ ) of 40 °C, the expected lifetime ( $t_f$ ) of NBR is estimated from Toop's (Toop 1971) table by using Equation (24)

$$\log(t_f) = \frac{E_a}{2.303RT_f} + \log\left(\frac{E_a}{R\alpha} \times P(\chi)\right) \quad (24)$$

**Fig. 1** Dog-bone Specimens of NBR



## 2 Experimental section

This study examines the aging of NBR beams over a two-year period under natural laboratory conditions, with no load applied, at an average temperature of 32 °C and relative humidity of 50%. The study compares virgin NBR samples with the same chemical composition as the aged samples. Three samples were collected from different locations to ensure accurate results. The mechanical properties were evaluated using static structural tensile tests. DMA tests were used to analyze the viscoelastic properties of the beams. FTIR spectroscopy was used to identify changes in functional groups with aging. TGA tests were used to determine the activation energy and pre-exponential factor, which were used to estimate the NBR's shelf life. An unconstrained sandwich beam with an aluminum base was used to conduct damping tests.

### 2.1 Static structural tests

#### 2.1.1 Tensile test

Dog-bone shape (ISO 37:2011) specimens, as shown in Fig. 1, were used to conduct tensile tests on a universal tensile testing machine (UTM: SDTRX-10 KN, Deepak Poly Plast, India) at a rate of 50 mm/min to determine the elastic modulus, elongation break, % of elongation, tensile strength, and maximum tensile strength. The load-cell accuracy was  $\pm 0.5\%$  of the total applied load at room temperature.

#### 2.1.2 Hardness test

The surface hardness of the virgin and aged NBR was measured using a Shore – A hardness tester (ISO 7619-1:2010). Tests were conducted on the surface of the samples at different locations, and an average was taken to obtain accurate data.

#### 2.1.3 Density tests

With age, the crystalline and amorphous phases of the polymer change, which results in crosslink density and, hence, specific gravity. Specific gravity tests (Deepak Poly Plast, India) were conducted according to ISO 1183-1:2019 using a digital density meter. Pure water with a density of 1000 kg/m<sup>3</sup> was used as reference. The accuracy of the digital density meter is 0.1 kg/m<sup>3</sup>.

## 2.2 Dynamic Mechanical Analysis (DMA)

DMA tests were used to determine the frequency-dependent constitutive viscoelastic properties of virgin and naturally aged NBR. The frequency domain data were fitted in the generalized Maxwell model ( $i = 3$  in Equation (12)) and converted to the time domain using Equations (11) and (12). Because the response of the viscoelastic material during vibration absorption is in the shear mode, the tests were carried out in the compressive mode. Cylindrical samples with diameters of 5 mm were carefully cut from virgin and naturally aged beams. The storage modulus ( $G'$ ), loss modulus ( $G''$ ), and loss factor ( $\tan \delta$ ) in shear mode were measured using a Dynamic Mechanical Analyzer (EXSTAR 6000, Seiko Instruments Inc., Japan) at various frequencies and sweep temperatures. The testing temperature ranged from 30 °C to 108 °C with frequencies of 0.1 Hz, 0.5 Hz, 1 Hz, 5 Hz, and 10 Hz. The oscillation amplitude is  $\pm 0.5$  mm.

## 2.3 Fourier Transformed Infrared Spectrophotometry (FTIR)

FTIR spectroscopy was used to describe the functional groups of the polymers. A germanium ATR (Cary 630 FTIR Spectrometer, Agilent, USA) was used to capture 64 spectra at the center of the beam cross section. Tests were performed in the 650  $\text{cm}^{-1}$  to 4000  $\text{cm}^{-1}$  wavelength range at room temperature.

## 2.4 Thermogravimetric Analysis (TGA)

The thermal decomposition of the polymers follows first-order kinetic (Toop 1971). To obtain the degradation regions, the polymers were heated at different heating rates using TGA (Q600 SDT, TA Instruments, USA). To avoid oxidation, the samples (10 mg  $\sim$  15 mg) were heated in a nitrogen environment at rates of 5 °C/min, 10 °C/min, 15 °C/min, and 20 °C/min with a purge flow of 100 ml/min. The testing temperature range is up to 700 °C from room temperature. The derivative weight percentage was calculated using Equation (25).

$$\text{Derivative weight \%ge} = \left[ \frac{w_o - w_f}{w_i - w_f} \right] \times 100 \quad (25)$$

where  $w_o$  is the actual weight of the sample,  $w_i$  is the initial weight, and  $w_f$  is the final weight (mg).

From the TGA experimental data, model-free kinetic methods (see Sect. 1.3) were used to calculate the frequency factor or pre-exponential factor and activation energy at different conversion rates, and shelf life was estimated using the Toops equation (Equation (24) in Sect. 1.4).

## 2.5 Damping tests

The study aimed to investigate the degradation of NBR material's damping capacity over time by conducting damping tests on an unconstrained sandwich beam made of virgin and naturally aged NBR, with aluminum as the base material. The beam was mounted on an electrodynamic shaker (Sdyn SEV 360, Saraswati Dynamics Pvt. Ltd., India) and tested in a frequency range of 20 Hz to 1000 Hz with different levels of base amplitude excitation as shown in Fig. 2. Acceleration was measured using an accelerometer, and the responses were captured at three different locations. To ensure accuracy, three trials were conducted for each sample, and the data were analyzed using Fast Fourier Transformation.



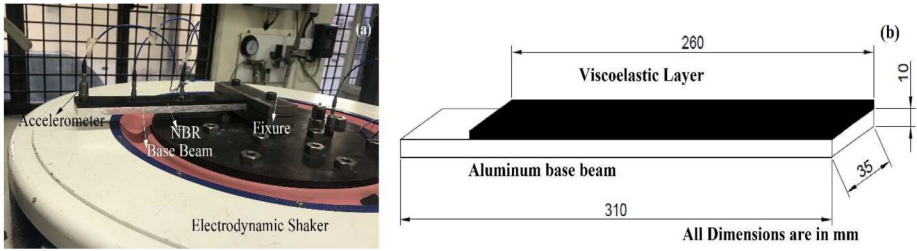
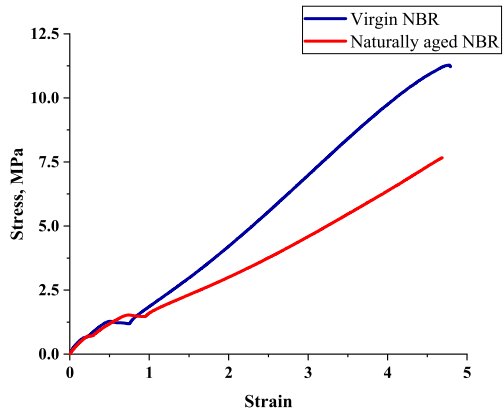


**Fig. 2** (a) Electrodynamic shaker with cantilever fixture (b) Unconstrained Viscoelastic sandwich beam

**Table 1** Mechanical Properties of NBR

Parameter	Virgin NBR	Naturally aged NBR	%ge of deterioration
Tensile strength (MPa)	5.26 ± 0.51	3.03 ± 0.43	42.39
Maximum tensile strength (MPa)	11.35 ± 0.08	6.65 ± 0.54	41.41
Elastic Modulus (MPa)	2.18 ± 0.15	1.17 ± 0.16	46.33
%ge of Elongation break	478.2 ± 16.92	424.16 ± 25.08	11.30
Hardness (Shore – A)	84.6 ± 1.14	83.4 ± 1.15	1.42
Density (kg/m <sup>3</sup> )	1417.3 ± 23.4	1252.3 ± 26.12	11.64

**Fig. 3** Stress vs Strain of NBR



### 3 Results and discussion

#### 3.1 Static structural tests

The mechanical properties (static) of the naturally aged NBR and virgin NBR were evaluated using the uniaxial tensile test, shore – A hardness test, and digital density meter, as shown in Table 1.

Fig. 3 depicts the stress vs strain of the NBR. The mechanical properties of NBR deteriorate significantly after two years of natural aging. The tensile strength, maximum tensile strength, and elastic modulus of NBR decrease by approximately 43.4%, 41.4%, and 46.3%,

**Table 2** Dynamic Mechanical Properties of NBR at 40°C

Sample	Frequency, Hz	Storage Modulus ( $G'$ ), MPa	Loss Modulus ( $G''$ ), MPa	Loss factor ( $\tan \delta$ )
Virgin NBR	0.1	7.863	1.215	0.154
	0.5	9.708	1.535	0.158
	1	10.713	1.746	0.163
	5	14.148	2.376	0.167
	10	15.496	2.680	0.172
Aged NBR	0.1	4.524	0.472	0.104
	0.5	5.008	0.528	0.105
	1	5.226	0.570	0.109
	5	5.835	0.717	0.122
	10	6.113	0.807	0.132

respectively. However, the percentage of elongation break only decreased by 11.3%. The density decreased by 11.6%, and the surface hardness did not change much.

The mechanical properties of NBR deteriorate with aging due to changes in the polymer crosslinking degree. The changes in crosslinking degree cause for decrease in elongation break, although not significant, is a result of natural oxidative aging. The loading rate during testing, conducted at a slower rate of 50 mm/min, also affects the elongation break. The surface hardness remains mostly unchanged, but major mechanical properties such as tensile strength, maximum tensile strength, and elastic modulus decrease by over 40% after two years. This is caused by an increase in crosslink density, which leads to a decrease in the molar mass between crosslink points and chain mobility, resulting in stress concentration and decreased basic mechanical properties. The density of the material may also change slightly due to volumetric relaxation and rearrangement of molecular structures in the amorphous phase during aging (Liu et al. 2016; Zhao et al. 2015).

### 3.2 Dynamic Mechanical Analysis (DMA)

The strength and stability of polymeric materials cannot be fully determined through static tests alone. The dynamic viscoelastic properties of the materials that change with frequency were evaluated using DMA and the results are shown in Table 2. The data collected was then fit in GMM using a curve-fitting technique. The storage modulus data was used specifically for this purpose as the loss modulus value was relatively small in comparison and the loss factor values were close to zero. By using the storage modulus data, it was possible to approximate the Maxwell constants well. The third-order Maxwell equation provided the best fit for the data, with  $R$  (Bendjaouahdou and Bensaad 2018) value of 0.99. The results were then used to determine the Maxwell constants and relaxation strength. Figs. 4 and 5 show the changes in the storage modulus and dynamic mechanical properties of virgin and aged NBR at 40 °C, respectively. The constants of the third order Maxwell model are listed in Table 3.

The variations in the dynamic mechanical properties with temperature are shown in Figs. 6 and 7. The loss modulus ( $G''$ ) and loss factor ( $\tan \delta$ ) of the naturally aged NBR decreased up to 80 °C and then increased again. In contrast, the dynamic mechanical properties of virgin NBR decreased continuously even after 80 °C. It can be observed from Fig. 6

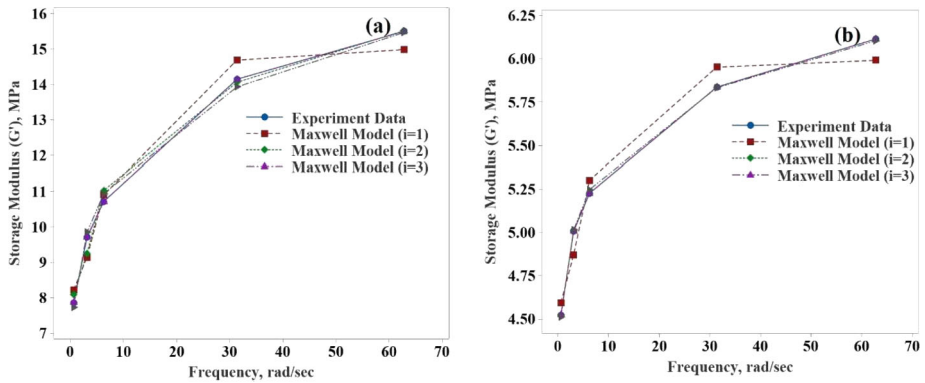


**Fig. 4** Storage Modulus vs frequency of (a) Virgin NBR (b) naturally aged NBR at 40 °C

**Table 3** Maxwell constants with  $I = 3$  ( $G$ : mPa,  $\tau$ : sec) at 40 °C

Sample	$G_e$	$G_1$	$\tau_1$	$G_2$	$\tau_2$	$G_3$	$\tau_3$
Virgin NBR	7.660	3.077	0.419	4.236	0.045	1.291	0.028
Naturally Aged NBR	4.443	0.941	0.034	0.611	0.601	0.289	0.191

that a small inflection point is formed at 80 °C, resulting in a change in the slope of the loss modulus line. This indicates that the aged NBR becomes more softer after 80 °C and molecular motions increase, but the complete flow is hindered by the chemical crosslinks, leading to an increase in the loss factor and damping properties. The changes in crosslinking degree observed in aged NBR are the cause for the property changes, which do not occur in virgin NBR.

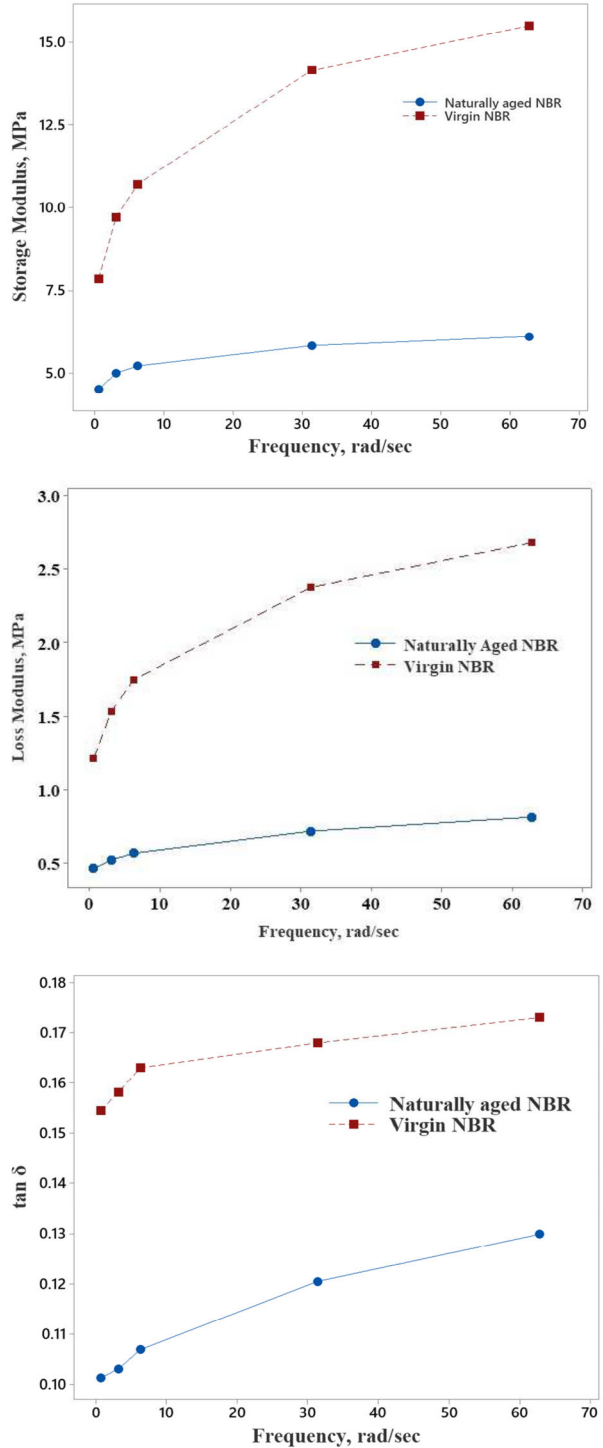
The relaxation modulus of virgin and naturally aged NBR was calculated using Equation (12) and plotted in Fig. 8. It was observed that when a load was applied for a longer duration, the relaxation modulus tended to  $G_e$ . The virgin NBR took less time to relax at 80 °C, and more time to relax at temperatures below and above 80 °C. On the other hand, the naturally aged NBR took less time to relax at temperatures below 100 °C, but took longer to relax at higher temperatures. This was attributed to a slight change in the surface hardness caused by aging.

### 3.3 FTIR

The FTIR tests were carried out at room temperature to capture waveband spectra of functional groups. Fig. 9 depicts how NBR wavebands change with age.

The peaks observed at 2914.7  $\text{cm}^{-1}$  in the FTIR spectrum of NBR correspond to the C–H stretching vibrations of aliphatic groups found in the butadiene segments of the polymer. The peak at 1722  $\text{cm}^{-1}$  is associated with the C=O stretching vibrations of the nitrile groups ( $-\text{C}\equiv\text{N}$ ) present in the acrylonitrile segments of the NBR polymer. The peak at 1423.84  $\text{cm}^{-1}$  is due to the C–H bending vibrations of the aliphatic groups found in the butadiene segments. The peak at 1654.9  $\text{cm}^{-1}$  is attributed to the C=C stretching vibrations of the conjugated double bonds in the butadiene segments. The peak at 1110.74  $\text{cm}^{-1}$  corresponds to the C–N stretching vibrations of the nitrile groups ( $-\text{C}\equiv\text{N}$ ) present in the acrylonitrile segments. The peak at 961.65  $\text{cm}^{-1}$  is related to the C–H bending vibrations of the

**Fig. 5** Variation of viscoelastic properties with frequency of virgin and aged NBR at 40 °C temperature



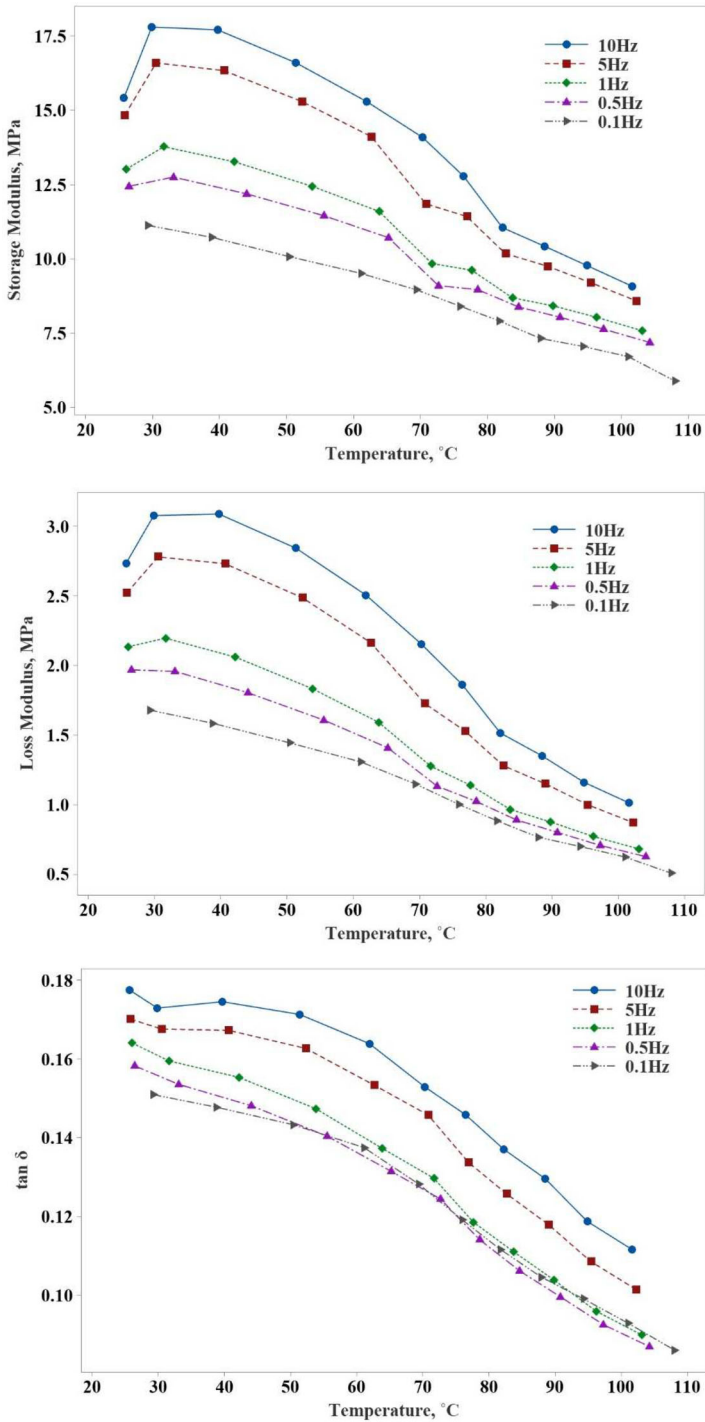


Fig. 6 Variation of viscoelastic properties with temperature of virgin NBR

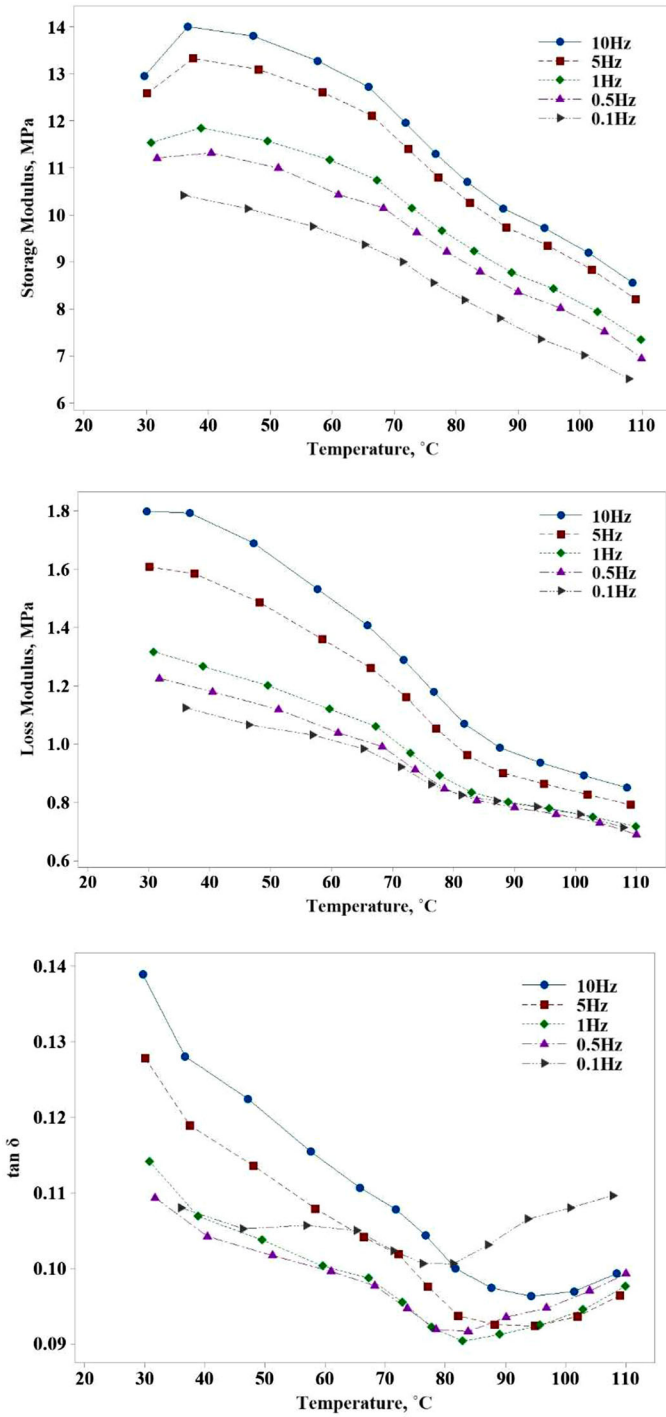
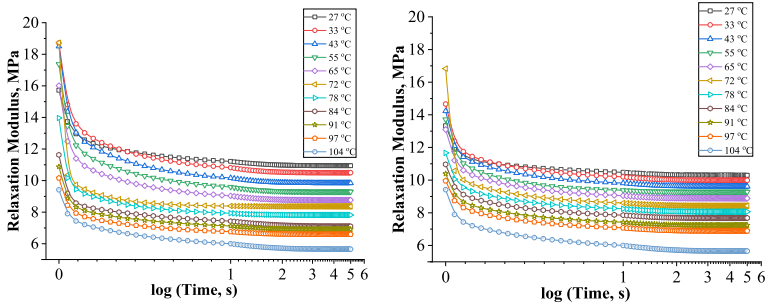
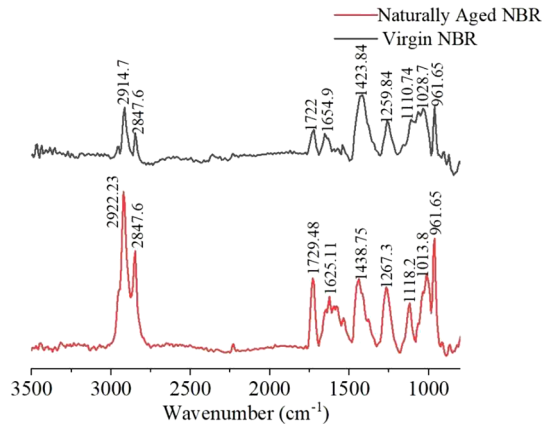


Fig. 7 Variation of viscoelastic properties with temperature of naturally aged NBR



**Fig. 8** Relaxation modulus vs time for (a) virgin NBR (b) naturally aged NBR

**Fig. 9** FTIR spectra of virgin and aged NBR



aliphatic groups found in the butadiene segments, and this peak intensity did not change significantly with natural aging in an oxidative environment. Finally, the peak at  $1259.84\text{ cm}^{-1}$  is assigned to the C–N bending vibrations of the nitrile groups ( $-\text{C}\equiv\text{N}$ ) present in the acrylonitrile segments of the NBR polymer.

As NBR ages, it undergoes various chemical reactions, such as oxidation, hydrolysis, and crosslinking, which can alter the chemical composition of the material and lead to changes in the peak intensities. These reactions can lead to the formation of new chemical groups, such as carbonyl or carboxyl groups, and can also lead to the degradation of existing groups, such as the C=C double bonds in the polymer backbone. These changes can result in new peaks appearing in the FTIR spectrum or changes in the intensity of existing peaks, depending on the specific chemical reactions that take place (Zhao et al. 2013; Sadeghalvaad et al. 2019; Azevedo et al. 2018).

### 3.4 Thermal analysis

TGA tests were performed in a non-reactive nitrogen environment to estimate the shelf life of the NBR. The activation energy calculated from the TGA spectra was used to calculate shelf life. The samples in this study were heated at four different rates:  $5\text{ }^\circ\text{C}/\text{min}$ ,  $10\text{ }^\circ\text{C}/\text{min}$ ,  $15\text{ }^\circ\text{C}/\text{min}$ , and  $20\text{ }^\circ\text{C}/\text{min}$ . To prevent oxidation during heating, a purge flow of  $100\text{ ml}/\text{min}$  of nitrogen is supplied to the heating chamber. TGA provides thermogravimetric (TG) and Derivative Thermogravimetric (DTG) decomposition profile curves for naturally aged NBR

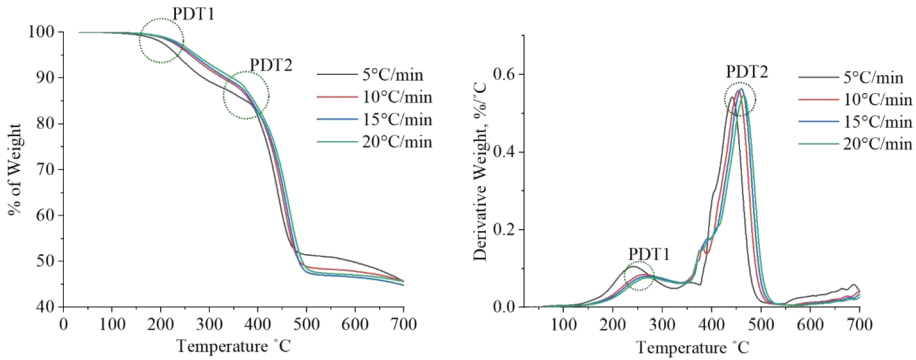


**Fig. 10** TGA and DTG spectra for virgin NBR

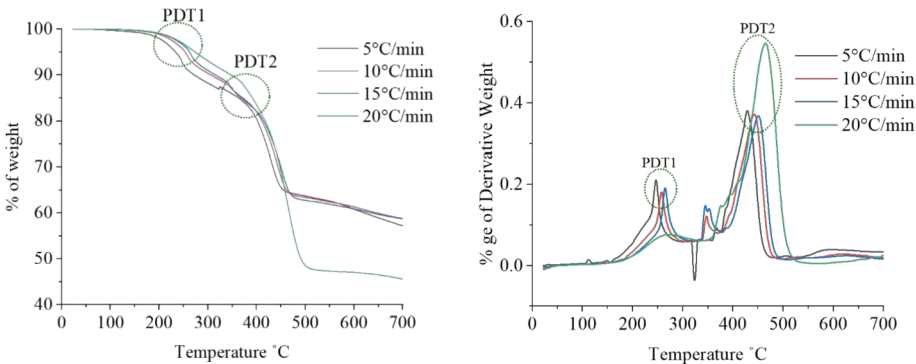


**Fig. 11** TGA and DTG spectra for naturally aged NBR

and virgin NBR. NBR's TG and DTG profiles of NBR are shown in Figs. 10 and 11, respectively. The peak degradation of NBR occurred at two temperatures: PDT1 and PDT2. At a heating rate of 5 °C/min, the virgin NBR lost 5.75% of its weight and aged NBR lost 7.57% at PDT1. This is because the volatile compounds and additives in NBR evaporate. For the same heating rate, the substantial weight loss for the virgin NBR is 35.64%, and that for the aged NBR is 28.34% at PDT2. This was due to polymer pyrolysis and carbon black combustion.

For all heating rates, PDT1 ranges from 215 °C to 285 °C for both virgin and aged NBR, whereas PDT2 ranges from 415 °C to 495 °C for virgin NBR and 385 °C to 485 °C for aged NBR. Figs. 10 and 11 illustrate how aged NBR loses weight at lower temperatures than virgin NBR at PDT1 owing to the early vapor of volatile components. Aged NBR, on the other hand, exhibits less weight loss at 700 °C than virgin NBR owing to the formation of new crosslinking point with aging. Nonetheless, at higher heating rates, that is, 20 °C/min, aged NBR degrades nearly identically to virgin NBR. These findings are consistent with those of FTIR spectroscopy.

### 3.4.1 Activation energy

The activation energy can be used to characterize polymer degradation and durability. The activation energy was calculated in this study by plotting the logarithm of the heating rate



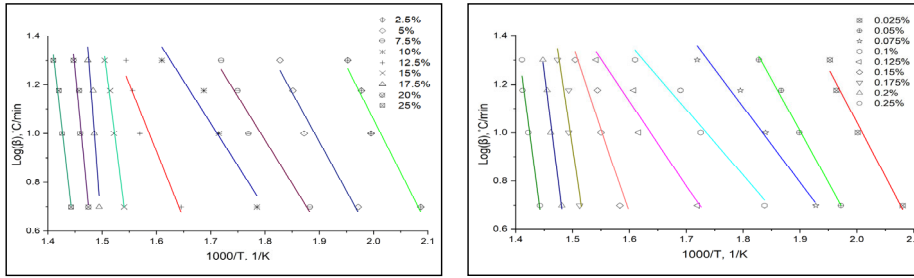


Fig. 12 OFL plots of (a) virgin NBR (b) naturally aged NBR

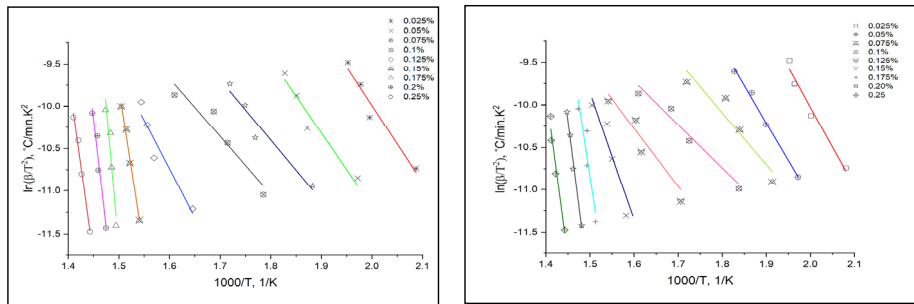


Fig. 13 KAS plots of (a) virgin NBR (b) naturally aged NBR

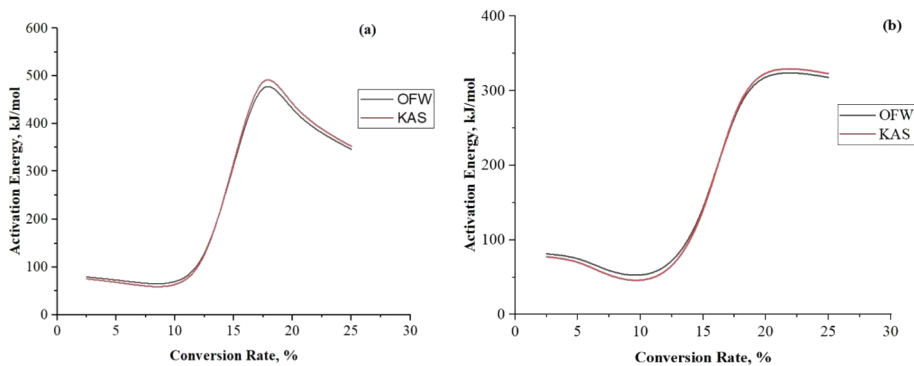


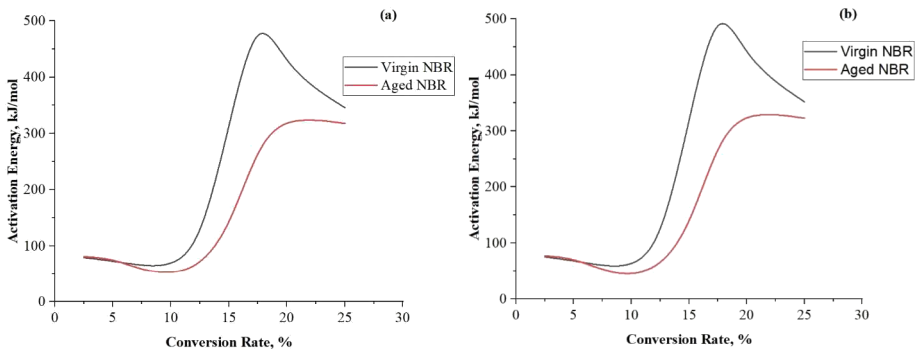
Fig. 14 Variation in activation energy vs conversion rate of (a) virgin NBR (b) aged NBR

vs. the reciprocal of temperature, using model-free kinetic methods such as Ozawa-Flynn-Wall (OFW) and Kissinger-Akahira-Sunose (KAS) (Ozawa 1965; Zhu et al. 2015; Flynn and Wall 1966; E37 Committee 2018). The slopes of the plots are shown in Figs. 12–13 and fitted to be linear to calculate and activation energy using Equations (20) and (23). Table 4 lists the frequency factors ( $\log(A), \text{min}^{-1}$ ) and activation energies calculated using model-free kinetic methods at various conversion rates.

The variation of activation energy in virgin NBR and aged NBR with conversion rate is shown in Figs. 14 and 15. The two modal free kinetic methods, OFW and KAS, used in the

**Table 4** Activation energy and frequency factor of virgin and aged NBR

Conversion factor	Ozawa-Flynn-Wall (OFW)				Kissinger-Akahira-Sunose (KAS)			
	$E_a$ , kJ mol <sup>-1</sup>		Log (A), min <sup>-1</sup>		$E_a$ , kJ mol <sup>-1</sup>		Log (A), min <sup>-1</sup>	
	Virgin	Aged	Virgin	Aged	Virgin	Aged	Virgin	Aged
2.5%	79.39	78.25	4.24	4.33	75.32	74.26	3.52	3.71
5%	73.33	72.57	3.74	3.95	68.43	67.88	2.48	2.79
7.5%	65.00	56.83	3.21	2.92	59.19	50.63	1.38	0.37
10%	63.36	49.39	3.02	2.48	56.87	42.33	1.01	-0.68
12.5%	100.16	63.75	4.22	2.92	94.99	56.84	3.47	0.28
15%	312.29	128.82	11.78	5.20	317.70	124.72	19.25	5.49
17.5%	529.77	280.15	19.22	10.43	546.26	283.66	34.80	17.51
20%	411.46	331.35	14.79	12.01	421.60	337.33	25.47	21.12
25%	345.78	317.81	12.21	11.24	352.20	322.77	20.15	19.32
Average	237.64	153.21	8.49	6.164	221.39	151.15	12.39	7.767

**Fig. 15** Variation of activation energy vs conversion rate by (a) OFL and (b) KAS methods

present study are congruent. In both virgin and aged NBR, the activation energy decreases marginally up to a 10% conversion rate, and then increases to a 17.5% conversion rate; thereafter, it decreases. This implied that the energy required to break the polymer chains during the thermal degradation process was between 10% and 17.5% conversion rate. Correspondingly, the maximum activation energies of 530 kJ mol<sup>-1</sup> for virgin NBR and 332 kJ mol<sup>-1</sup> for aged NBR were observed at a 17.5% conversion rate. The frequency factor, also known as the pre-exponential factor log(A), determines the frequency of molecular interactions and thus the polymer groups within reach for thermal decomposition (Batista et al. 2015). The frequency factor was smaller at the initial stages of the degradation process, indicating that fewer hydrocarbons were available to participate in the reaction process. Thermal decomposition of NBR accelerates as it heats up, causing an increase in polymer chain scissions and, consequently, degradation processes. It was also observed that the frequency factor was higher when the activation energy was higher. The activation energy and shelf life of polymers are directly proportional (Ammineni et al. 2022). Aged NBR has a lower activation energy than virgin NBR, which means that less energy is required to initiate the reaction at high conversion rates. Therefore, the design engineer must not overlook the kinetic parameters of polymeric seals or dampers when designing for long service life. The OFW and KAS

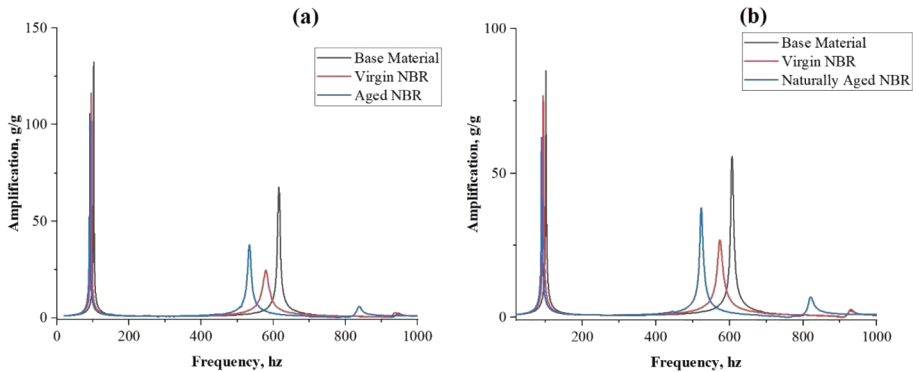


**Fig. 16** First three fundamental frequencies of beams at (a) 0.1 g, and (b) 1 g base excitation

approaches yielded the same range of activation energies. Because the kinetic parameters tested in the laboratory were in an inert nitrogen atmosphere, the results may vary slightly in real-time applications (Dhaundiya and Hanon 2018).

The shelf life of the NBR was estimated using the Toops equation (see Sect. 1.4) at a conversion rate of 5% (Toop 1971). At an operating temperature of 40 °C, the activation energy and corresponding shelf life of virgin NBR are 73.33 kJ mol<sup>-1</sup> and 17.32 years. The aged NBR, on the other hand, has an activation energy of 72.57 kJ mol<sup>-1</sup> and corresponding shelf life is 14.63 years. However, the shelf life of an NBR is estimated in an inert environment with no mechanical load. Because NBR seals and dampers operate in hazardous environments with mechanical loads in many applications, their expected life may vary accordingly. As a result, the environmental conditions and applied loads may accelerate the pyrolysis process, causing further degradation of the service life.

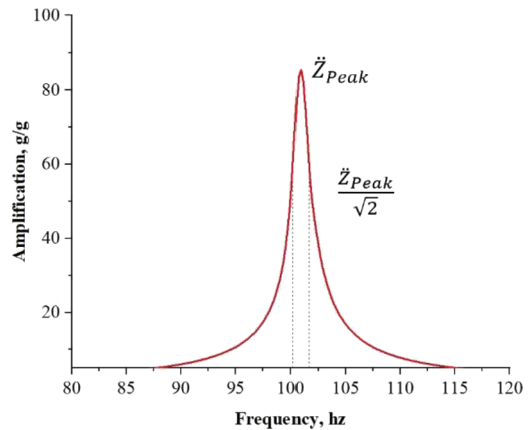
### 3.5 Damping tests

A dynamic shaker was used to perform dynamic tests on the cantilever beams. The frequency response was recorded at three different locations for sinusoidal harmonic base excitation at 1 g and 0.1 g amplitudes (Fig. 16). The accelerometers capture the frequency responses of the base beam and the unconstrained sandwich beam with virgin and aged NBR in the first three modes. Because the maximum amplitude of displacement is at the beam tip, it was considered for further analysis. The response of the beam at the tip is shown in Fig. 16. The response amplification values as well as the corresponding natural frequencies, quality factors, damping ratios, and loss factors are listed in Table 5.

The fundamental frequencies and amplitudes of the vibrations in the base beam are significantly reduced owing to the additional contribution of mass and damping by the viscoelastic layer. The aged NBR beam had a lower excitation frequency than the virgin NBR and the base beam. The elastic nature of the NBR decreases with age; thus, the excitation frequency is lower than that in the virgin NBR beam. The amplitude of vibration is significantly lower at the first natural frequency by adding aged NBR rather than virgin NBR to the base aluminum beam, however, at the second and third natural frequencies, the amplitude of vibration is higher for aged NBR rather than virgin NBR layer. Regardless of the type of beam material, the amplitude of the base excitation had no effect on the fundamental frequencies, however, the amplification factor was significantly affected by the amplitude of excitation. At 1 g amplitude of excitation, natural frequencies of virgin material are

**Table 5** Modal values of beams for the first three natural frequencies at 0.1 g and 1 g

		Frequency, Hz	Amplification, g/g	$Q$	$\xi$	$\eta$
1 g Amplitude of excitation						
Base Material	Mode 1	100.93	85.85	70.938	0.0061	0.0123
	Mode 2	607.29	55.831	85.07	0.00591	0.0118
	Mode 3	930	2.7005	62.986	0.00796	0.0159
Virgin NBR	Mode 1	93.504	77.583	58.911	0.0085	0.0171
Sandwich Beam	Mode 2	573.45	26.867	44.23	0.01144	0.0228
	Mode 3	928.22	2.2531	46.12	0.0108	0.0216
Aged NBR	Mode 1	88.802	62.979	62.195	0.0078	0.0157
Sandwich Beam	Mode 2	523.18	38.163	66.979	0.0075	0.0150
	Mode 3	821.36	7.0272	59.683	0.00834	0.0166
0.1 g Amplitude of excitation						
Base Material	Mode 1	101.9	133.7	72.457	0.00716	0.0143
	Mode 2	615.46	67.237	90.531	0.00543	0.0108
	Mode 3	946.13	2.4042	67.34	0.00746	0.0149
Virgin NBR	Mode 1	94.764	117.96	62.02	0.0082	0.0015
Sandwich Beam	Mode 2	578.95	24.687	38.807	0.0129	0.0259
	Mode 3	937.13	2.5905	58.91	0.00819	0.0163
Aged NBR	Mode 1	91.036	107.34	70.13	0.00713	0.0142
Sandwich Beam	Mode 2	533.28	37.762	60.608	0.00806	0.0161
	Mode 3	838.81	5.8992	65.783	0.00777	0.0155

**Fig. 17** First natural frequency of base beam at tip

93.504 Hz, 573.45 Hz and 928.22 Hz, whereas aged material has 88.802 Hz, 523.18 Hz, and 821.36 Hz.

3 dB method was used to determine the effective damping constant of the viscoelastic sandwich beams at resonance frequencies. Fig. 17 shows the peak amplitude of the base aluminum beam at its first natural frequency. The corresponding 3 dB points were determined using the peak resonance amplitude and the offset of  $\frac{1}{\sqrt{2}}$  the peak amplitude at the

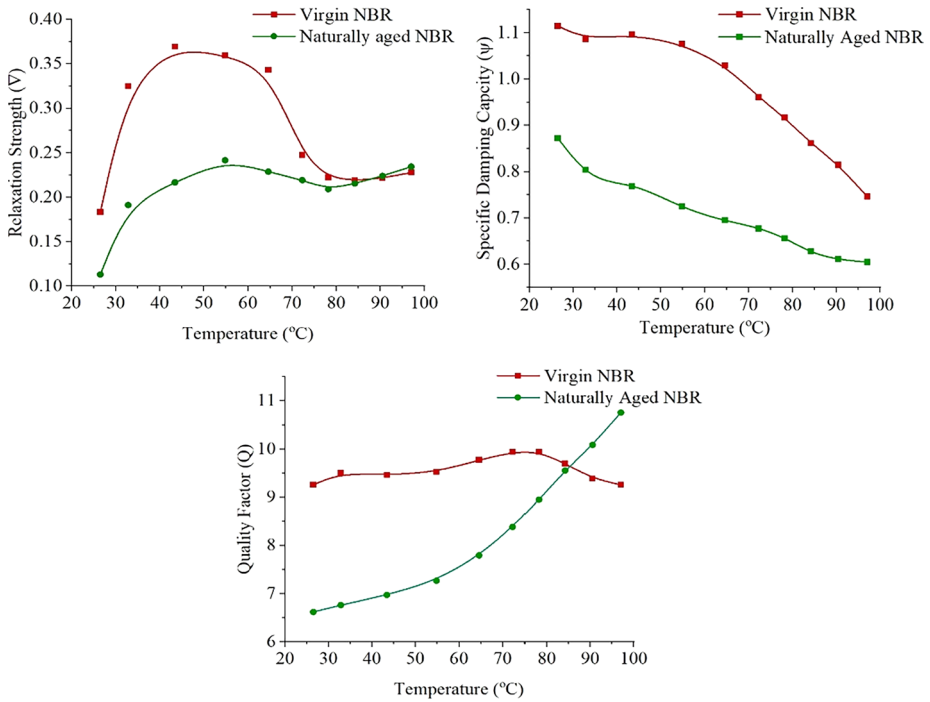


**Fig. 18** Relaxation strength, specific damping capacity and quality factor vs temperature of NBR

two sides of the curve from the peak (Ammineni et al. 2022). Equations (8) and (9) can be used to calculate the effective damping factor ( $\xi$ ) and loss factor ( $\eta$ ) of the sandwich beam. As NBR ages, the cross-linking density can decrease and the polymer chains can become more mobile, which can result in a decrease in the material’s damping ability. Additionally, exposure to oxidative environment can cause degradation of the polymer chains and cross-links, further contributing to a decrease in damping ability. At lower natural frequencies, on the other hand, the material has enough time to relax and exhibit a higher amplitude of vibrations than aged NBR. For low-amplitude base excitations, aged NBR has no greater effect on vibration damping than virgin NBR does. Because of the lack of free, entangled molecular chains in NBR, which prevents it from holding sufficient time to relax at higher frequencies, the effective damping ratio and loss factor of a virgin NBR sandwich beam decreased with age by 8% at the first resonance frequency and by 34% at the second resonance frequency. The damping parameters listed in Table 5 are actual characteristics that also consider the base aluminum material.

The temperature has a significant impact on the damping capacity of polymeric materials. The relationships between the damping parameters, temperature, and age are shown in Fig. 18. Up to 70 °C, the relaxation strength of virgin NBR was noticeably higher than that of aged NBR; however, after that point, its values abruptly decreased. Because both materials soften after 80 °C, the relaxation strengths of virgin NBR and aged NBR were the same. Temperature had a greater impact on virgin NBR than on aged NBR. Fig. 18 also shows how the stiffness and damping capacity of NBR materials degrade over time and with temperature.

In addition to the relaxation strength, two other parameters that determine NBR's damping ability of the NBR are specific damping capacity ( $\Psi$ ) and quality factor ( $Q$ ). The specific damping capacity of the virgin NBR is steady up to 60 °C before rapidly declining with temperature. The specific damping capability of naturally aged NBR decreased steadily with temperature. Although its specific damping ability rapidly decreases at higher temperatures, virgin NBR dampens vibrations more quickly than aged NBR. However, the quality factor of virgin NBR is almost constant with temperature at resonance frequencies, indicating that at higher temperatures, virgin NBR dissipates energy more quickly than aged NBR. On the other hand, the quality factor of naturally aged NBR increases with temperature, implying that its potential to dissipate energy diminishes with aging and temperature.

## 4 Conclusions

The present study investigates the effects of time and temperature on NBR's mechanical performance degradation of NBR. Numerous static and dynamic mechanical tests were performed to evaluate the deterioration in the mechanical and modal performance. The constitutive viscoelastic properties with time and temperature were obtained by fitting the experimental data with a generalized Maxwell model of higher order. To investigate how NBR degrades, TGA and FTIR measurements were performed. The following are the most significant observations.

- In two years, the fundamental mechanical properties, such as the tensile strength and elastic modulus, decreased by 40% when there was no load.
- Time and temperature have a significant impact on NBR's modal parameters of NBR, which decrease by approximately 50%.
- The modal frequencies and amplitude ratios of the NBR deteriorated by 8% at the first natural frequency and 30% at higher resonance frequencies.
- According to DMA studies, the constitutive viscoelastic characteristics of NBR are significantly influenced by temperature and rapidly decrease above 40 °C.
- The activation energy of aged NBR obtained from TGA and model-free kinetic analysis was considerably lower than that of the virgin NBR.
- The OFW and KAS model-free kinetic approaches showed good agreement in determining the activation energy and pre-exponential factors.
- The shelf life of naturally aged NBR is 14.63 years, compared to 17.32 years for virgin NBR.
- At 40 °C, NBR's energy dissipation capacity ( $\Psi$ ) during vibration absorption was reduced by 34% with age.
- The relaxation strengths of virgin and aged NBR are the same, as the NBR softens above 80 °C.
- The specific damping capacity degraded by 34% at lower excitation frequencies and by 25% at higher frequencies.
- In the temperature range of 40–80 °C, the temperature had little impact on the quality factor of the virgin NBR.

**Author contributions** Author Contribution Category 1 Conception and design of study: Syam Prasad Ammineni, D. Linga Raju, Ch. Nagaraju. Acquisition of data: Syam Prasad Ammineni, D. Linga Raju, Ch. Nagaraju. Analysis and/or interpretation of data: Syam Prasad Ammineni, D. Linga Raju, Ch. Nagaraju. Category 2 Drafting the manuscript: Syam Prasad Ammineni. Revising the manuscript critically for important intellectual content: Syam Prasad Ammineni, D. Linga Raju, Ch. Nagaraju. Category 3 Approval of the version of the manuscript to be published (the names of all authors must be listed): Syam Prasad Ammineni, D. Linga Raju, Ch. Nagaraju.

**Funding** The authors did not receive support from any organization for the submitted work. No funding was received to assist with the preparation of this manuscript. No funding was received for conducting this study. No funds, grants, or other support were received.

## Declarations

**Competing interests** The authors declare no competing interests.

## References

- Abdullah, N.A.S., Abdullah, F.F., Sufian, A.H., Abidin, A.N.S.Z., Jamaludin, A.S., Razali, M.N.M.: Effect of degradation by temperature onto nitrile rubber elastomer mechanical properties. *Mater. Today Proc.* **48**, 1941–1946 (2022). <https://doi.org/10.1016/j.matpr.2021.10.247>
- Akahira, T., Sunose, T.: Joint convection of four electrical institutes. *Sci. Technol.* **16**, 22–31 (1971)
- Ammineni, S.P., Nagaraju, C., Lingaraju, D.: Thermal degradation of naturally aged NBR with time and temperature. *Mater. Res. Express* **9**(6), 065305 (2022). <https://doi.org/10.1088/2053-1591/ac7302>
- Ammineni, S.P., Nagaraju, Ch., Raju, D.L.: Modal performance degradation of naturally aged NBR. *Polym. Test.* **115**, 107710 (2022). <https://doi.org/10.1016/j.polymertesting.2022.107710>
- Azevedo, J.B., Murakami, L.M.S., Ferreira, A.C., Diniz, M.F., Silva, L.M., Dutra, R. de C.L.: Quantification by FT-IR (UATR/NIRA) of NBR/SBR blends. *Polimeros* **28**, 440–449 (2018). <https://doi.org/10.1590/0104-1428.00918>
- Batista, N.L., Costa, M.L., Iha, K., Botelho, E.C.: Thermal degradation and lifetime estimation of poly(ether imide)/carbon fiber composites. *J. Thermoplast. Compos. Mater.* **28**(2), 265–274 (2015). <https://doi.org/10.1177/0892705713484740>
- Baumgaertel, M., Winter, H.H.: Determination of discrete relaxation and retardation time spectra from dynamic mechanical data. *Rheol. Acta* **28**(6), 511–519 (1989). <https://doi.org/10.1007/BF01332922>
- Bendjaouahdou, C., Bensaad S.: Aging studies of a polypropylene and natural rubber blend. *Int. J. Ind. Chem.* **9**(4), 345–352 (2018). <https://doi.org/10.1007/s40090-018-0163-2>
- Chakraborty, S., Bandyopadhyay, S., Ameta, R., Mukhopadhyay, R., Deuri, A.S.: Application of FTIR in characterization of acrylonitrile-butadiene rubber (nitrile rubber). *Polym. Test.* **26**(1), 38–41 (2007). <https://doi.org/10.1016/j.polymertesting.2006.08.004>
- Choi, S.-S., Kim, J.-C.: Lifetime prediction and thermal aging behaviors of SBR and NBR composites using crosslink density changes. *J. Ind. Eng. Chem.* **18**(3), 1166–1170 (2012). <https://doi.org/10.1016/j.jiec.2012.01.011>
- Corsaro, R.D., Sperling, L.H. (eds.): *Sound and Vibration Damping with Polymers*, ACS Symposium Series, vol. 424. American Chemical Society, Washington, DC (1990). <https://doi.org/10.1021/bk-1990-0424>
- Dhaundiyal, A., Hanon, M.M.: Calculation of kinetic parameters of the thermal decomposition of residual waste of coniferous species: cedrus deodara. *Acta Technol. Agric.* **21**(2), 75–80 (2018). <https://doi.org/10.2478/ata-2018-0014>
- Doyle, C.D.: Series approximations to the equation of thermogravimetric data. *Nature* **207**(4994), 290–291 (1965). <https://doi.org/10.1038/207290a0>
- E37 Committee: Test Method for Decomposition Kinetics by Thermogravimetry Using the Ozawa/Flynn/Wall Method, ASTM International (2018). <https://doi.org/10.1520/E1641-16>
- Esmaeili, R., Farhad, S.: Parameters estimation of generalized Maxwell model for SBR and carbon-filled SBR using a direct high-frequency DMA measurement system. *Mech. Mater.* **146**, 103369 (2020). <https://doi.org/10.1016/j.mechmat.2020.103369>
- Feng, J., Zhang, Q., Tu, Z., Tu, W., Wan, Z., Pan, M., Zhang, H.: Degradation of silicone rubbers with different hardness in various aqueous solutions. *Polym. Degrad. Stab.* **109**, 122–128 (2014). <https://doi.org/10.1016/j.polymdegradstab.2014.07.011>
- Ferry, J.D.: *Viscoelastic Properties of Polymers*. Wiley, New York (1980)
- Flynn, J.H., Wall, L.A.: A quick, direct method for the determination of activation energy from thermogravimetric data. *J. Polym. Sci. N* **4**(5), 323–328 (1966). <https://doi.org/10.1002/pol.1966.110040504>
- Funk, M., Parkin, S., Nieminen, T., Heckenberg, N., Rubinsztein-Dunlop, H.: Vaterite twist microrheology with AOM controlled optical tweezers. *Proc. SPIE Int. Soc. Opt. Eng.* **7227**, 72270D (2009). <https://doi.org/10.1117/12.814357>
- Ge, T., Huang, X.-H., Guo, Y.-Q., He, Z.-F., Hu, Z.-W.: Investigation of mechanical and damping performances of cylindrical viscoelastic dampers in wide frequency range. *Actuators* **10**(4), 71 (2021). <https://doi.org/10.3390/act10040071>

- Graesser, E.J., Wong, C.R.: The Relationship of Traditional Damping Measures for Materials with High Damping Capacity (1991). <https://apps.dtic.mil/sti/citations/ADA235347>. David Taylor Research Center Bethesda Md Ship Materials Engineering Dept, (accessed 2022-02-15)
- Gupta, Y.N., Chakraborty, A., Pandey, G.D., Setua, D.K.: Thermal and thermooxidative degradation of engineering thermoplastics and life estimation. *J. Appl. Polym. Sci.* **92**(3), 1737–1748 (2004). <https://doi.org/10.1002/app.20134>
- Hussain, M., Yasin, S., Memon, H., Li, Z., Fan, X., Akram, M.A., Wang, W., Song, Y., Zheng, Q.: Rheological and mechanical properties of silica/nitrile butadiene rubber vulcanizates with eco-friendly ionic liquid. *Polymers* **12**(11), 2763 (2020). <https://doi.org/10.3390/polym12112763>
- Jones, D.I.G.: Handbook of Viscoelastic Vibration Damping. Wiley, New York (2001)
- Jung, H., Song, H., Lee, M., Kim, Y., Youn, S., Lee, K., Shin, J., Kim, M.: Determination of viscoelastic properties of thin pressure sensitive adhesive using dynamic mechanical analysis. *Mech. Time-Depend. Mater.* **24**(2), 129–140 (2020). <https://doi.org/10.1007/s11043-019-09412-5>
- Kissinger, H.E.: Variation of peak temperature with heating rate in differential thermal analysis. *J. Res. Natl. Bur. Stand.* **57**(4), 217 (1956). <https://doi.org/10.6028/jres.057.026>
- Ko, Y.S., Forsman, W.C.: Dynamic mechanical testing of viscoelastic solids in free and forced oscillation: experiments with a modified weissenberg rheogoniometer. *Int. J. Polym. Mater. Polym. Biomater.* **8**(1), 53–63 (1980). <https://doi.org/10.1080/00914038008077934>
- Lakes, R.S.: Viscoelastic Materials. Cambridge University Press, Cambridge (2009)
- Li, B., Li, S., Shen, M., Xiao, Y., Zhang, J., Xiong, G., Zhang, Z.: Tribological behaviour of acrylonitrile-butadiene rubber under thermal oxidation ageing. *Polym. Test.* **93**, 106954 (2021). <https://doi.org/10.1016/j.polymertesting.2020.106954>
- Liu, J., Li, X., Xu, L., Zhang, P.: Investigation of aging behavior and mechanism of nitrile-butadiene rubber (NBR) in the accelerated thermal aging environment. *Polym. Test.* **54**, 59–66 (2016). <https://doi.org/10.1016/j.polymertesting.2016.06.010>
- Lyu, P., Li, W., Ma, Y., Cui, Y.: Effect of ageing on constrained damping structure of viscoelastic material. *AIP Conf. Proc.* **2036**(1), 030003 (2018). <https://doi.org/10.1063/1.5075656>
- Martinez-Agirre, M., Elejabarrieta, M.J.: Dynamic characterization of high damping viscoelastic materials from vibration test data. *J. Sound Vib.* **330**(16), 3930–3943 (2011). <https://doi.org/10.1016/j.jsv.2011.03.025>
- Maxwell, A.S., Broughton, W.R., Dean, G., Sims, G.D.: Review of Accelerated Ageing Methods and Lifetime Prediction Techniques for Polymeric Materials, National Physical Laboratory, London (2005)
- Musil, B., Johlitz, M., Lion, A.: On the ageing behaviour of NBR: chemomechanical experiments, modelling and simulation of tension set. *Contin. Mech. Thermodyn.* **32**(2), 369–385 (2020). <https://doi.org/10.1007/s00161-018-0728-5>
- Nait Abdelaziz, M., Ayoub, G., Colin, X., Benhassine, M., Mouwakeh, M.: New developments in fracture of rubbers: predictive tools and influence of thermal aging. *Int. J. Solids Struct.* **165**, 127–136 (2019). <https://doi.org/10.1016/j.ijsolstr.2019.02.001>
- Nakagawa, T., Toya, T., Oyama, M.: Ozone resistance of Highly Saturated Nitrile Rubber (HNBR). *J. Elastomers Plast.* **24**(3), 240–261 (1992). <https://doi.org/10.1177/009524439202400307>
- Ozawa, T.: A new method of analyzing thermogravimetric data. *Bull. Chem. Soc. Jpn.* **38**(11), 1881–1886 (1965). <https://doi.org/10.1246/bcsj.38.1881>
- Peng, Q., Zhu, Z., Jiang, C., Jiang, H.: Effect of stress relaxation on accelerated physical aging of hydrogenated Nitrile Butadiene Rubber using time-temperature-strain superposition principle. *Adv. Ind. Eng. Polym. Res.* **2**(2), 61–68 (2019). <https://doi.org/10.1016/j.aiepr.2019.03.002>
- Pertin, T., Minatchy, G., Adoue, M., Flory, A., Romana, L.: Investigation of nanoindentation as a fast characterization tool for polymer degradation study. *Polym. Test.* **81**, 106194 (2020). <https://doi.org/10.1016/j.polymertesting.2019.106194>
- Plota, A., Masek, A.: Lifetime prediction methods for degradable polymeric materials—a short review. *Materials* **13**(20), 4507 (2020). <https://doi.org/10.3390/ma13204507>
- Polukoshko, S.: Estimation of damping capacity of rubber vibration isolators under harmonic excitation. *Vibroeng. Proc.* **8**, 50–56 (2016)
- Qian, Y., Xiao, H., Nie, M., Zhao, Y., Luo, Y., Gong, S.: Lifetime prediction and aging behaviors of nitrile butadiene rubber under operating environment of transformer. *J. Electr. Eng. Technol.* **13**(2), 918–927 (2018). <https://doi.org/10.5370/JEET.2018.13.2.918>
- Rajesh, C., Divia, P., Dinooplal, S., Unnikrishnan, G., Purushothaman, E.: Dynamic mechanical analysis of nylon 6 fiber-reinforced acrylonitrile butadiene rubber composites. *Polym. Polym. Compos.* **29**(9\_suppl), S1328–S1339 (2021). <https://doi.org/10.1177/09673911211046144>
- Ranaei, O., Aghakouchak, A.A.: Experimental and numerical study on developed elastomeric layers based on natural and butyl matrix rubbers for viscoelastic dampers. *Mech. Time-Depend. Mater.* **26**(1), 211–233 (2022). <https://doi.org/10.1007/s11043-021-09484-2>



- Roylance, D.: Engineering Viscoelasticity (2001)
- Sadeghalvaad, M., Dabiri, E., Zahmatkesh, S., Afsharimoghadam, P.: Preparation and properties evaluation of nitrile rubber nanocomposites reinforced with organo-clay, CaCO<sub>3</sub>, and SiO<sub>2</sub> nanofillers. *Polym. Bull.* **76**(8), 3819–3839 (2019). <https://doi.org/10.1007/s00289-018-2583-8>
- Şen, M., Aksüt, D., Karaağaç, B.: The effect of ionizing radiation on the mechanical properties of NBR elastomers reinforced by lignin. *Radiat. Phys. Chem.* **168**, 108626 (2020). <https://doi.org/10.1016/j.radphyschem.2019.108626>
- Struik, L.: Physical Aging in Amorphous Polymers and Other Materials. Undefined (1978)
- Tang, Q.Y., Zhang, W.F.: Environmental factors on aging of Nitrile Butadiene Rubber (NBR) – a review. *Adv. Mater. Res.* **1033–1034**, 987–990 (2014). <https://doi.org/10.4028/www.scientific.net/AMR.1033-1034.987>
- Toop, D.J.: Theory of life testing and use of thermogravimetric analysis to predict the thermal life of wire enamels. *IEEE Trans. Electr. Insul.* **EI-6**(1), 2–14 (1971). <https://doi.org/10.1109/TEI.1971.299128>
- Tschoegl, N.W.: The Phenomenological Theory of Linear Viscoelastic Behavior: An Introduction. Springer, Berlin (1989)
- Vašina, M., Pöschl, M., Zádrapa, P.: A study of significant factors affecting viscoelastic damping properties of polymer materials. *Manuf. Technol.* **18**(3), 523–529 (2018). <https://doi.org/10.21062/ujep/132.2018/a/1213-2489/MT/18/3/523>
- Williams, M.L., Blatz, P.J., Schapery, R.A.: Fundamental Studies Relating to Systems Analysis of Solid Propellants. Defense Technical Information Center, Fort Belvoir, VA (1961). <https://doi.org/10.21236/AD0256905>
- Woo, C.S., Choi, S.S., Lee, S.B., Kim, H.S.: Useful lifetime prediction of rubber components using accelerated testing. *IEEE Trans. Reliab.* **59**(1), 11–17 (2010). <https://doi.org/10.1109/TR.2010.2042103>
- Xiong, Y., Chen, G., Guo, S., Li, G.: Lifetime prediction of NBR composite sheet in aviation kerosene by using nonlinear curve fitting of ATR-FTIR spectra. *J. Ind. Eng. Chem.* **19**(5), 1611–1616 (2013). <https://doi.org/10.1016/j.jiec.2013.01.031>
- Physical & Computational Science Directorate, Pacific Northwest National Laboratory, Richland, Washington 99354, United State; Zhang, X., Applications of kinetic methods in thermal analysis: a review. *Eng. Sci.* **14**, 1–13 (2020) <https://doi.org/10.30919/es8d1132>
- Physical & Computational Science Directorate, Pacific Northwest National Laboratory, Richland, Washington 99354, United State; Zhang, X.: Applications of kinetic methods in thermal analysis: a review. *Eng. Sci.* **14**, 1–13 (2020). <https://doi.org/10.30919/es8d1132>
- Zhang, J.X.J., Hoshino, K.: Chap. 6 – mechanical transducers: cantilevers, acoustic wave sensors, and thermal sensors. In: Edition, S., Zhang, J.X.J., Hoshino, K. (eds.) *Molecular Sensors and Nanodevices. Micro and Nano Technologies*, pp. 311–412. Academic Press, San Diego (2019). <https://doi.org/10.1016/B978-0-12-814862-4.00006-5>
- Zhao, J., Yang, R., Iervolino, R., Barbera, S.: Changes of chemical structure and mechanical property levels during thermo-oxidative aging of NBR. *Rubber Chem. Technol.* **86**(4), 591–603 (2013). <https://doi.org/10.5254/RCT.13.87969>
- Zhao, J., Yang, R., Iervolino, R., Barbera, S.: Investigation of crosslinking in the thermooxidative aging of Nitrile–Butadiene Rubber. *J. Appl. Polym. Sci.* **132**(3), 41319 (2015). <https://doi.org/10.1002/app.41319>
- Zheng, W., Zhao, X., Li, Q., Chan, T.W., Zhang, L., Wu, S.: Compressive stress relaxation modeling of butadiene rubber under thermo-oxidative aging. *J. Appl. Polym. Sci.* **134**, 12 (2017). <https://doi.org/10.1002/app.44630>
- Zhu, F., Feng, Q., Xu, Y., Liu, R., Li, K.: Kinetics of pyrolysis of ramie fabric wastes from thermogravimetric data. *J. Therm. Anal. Calorim.* **119**(1), 651–657 (2015). <https://doi.org/10.1007/s10973-014-4179-3>

**Publisher's Note** Springer Nature remains neutral with regard to jurisdictional claims in published maps and institutional affiliations.

Springer Nature or its licensor (e.g. a society or other partner) holds exclusive rights to this article under a publishing agreement with the author(s) or other rightsholder(s); author self-archiving of the accepted manuscript version of this article is solely governed by the terms of such publishing agreement and applicable law.